

PathRWKV: Enabling Whole Slide Prediction with Recurrent-Transformer

Sicheng Chen¹, Tianyi Zhang², Dankai Liao¹, Dandan Li¹, Low Chang Han³,
Yanqin Jiang¹, Yueming Jin^{2,3,*}, and Shangqing Lyu^{1,*}

¹ PuzzleAI Pte Ltd, Singapore 229594, Republic of Singapore
{sichengchen, dankailiao, dandanli, yanqinjiang,
shangqinglyu}@puzzleai.sg

² Department of Electrical & Computer Engineering, National University of
Singapore, Singapore 117417, Singapore
zhangtianyi@u.nus.edu

³ Department of Biomedical Engineering, National University of Singapore,
Singapore 117417, Singapore
e0543455@u.nus.edu, ymj@nus.edu.sg

Abstract. Pathological diagnosis plays a critical role in clinical practice, where the whole slide images (WSIs) are widely applied. Through a two-stage paradigm, recent deep learning approaches enhance the WSI analysis with tile-level feature extracting and slide-level feature modeling. Current Transformer models achieved improvement in the efficiency and accuracy to previous multiple instance learning based approaches. However, three core limitations persist, as they do not: (1) robustly address the modeling on variable scales for different slides, (2) effectively balance model complexity and data availability, and (3) balance training efficiency and inference performance. To explicitly address them, we propose a novel model for slide modeling, PathRWKV. Via a recurrent structure, we enable the model for dynamic perceptible tiles in slide-level modeling, which novelly enables the prediction on all tiles in the inference stage. Moreover, we employ linear attention instead of conventional matrix multiplication attention to reduce model complexity and overfitting problem. Lastly, we hinge multi-task learning to enable modeling on versatile tasks simultaneously, improving training efficiency, and asynchronous structure design to draw an effective conclusion on all tiles during inference, enhancing inference performance. Experimental results suggest that PathRWKV outperforms the current state-of-the-art methods in various downstream tasks on multiple datasets. The code and datasets are publicly available.

Keywords: Whole Slide Image Analysis · Multiple Instance Learning · Multiple Task Learning.

1 Introduction

Pathology diagnosis is crucial in clinical practice, with Whole Slide Images (WSIs) serving as the standard for pathological analysis [2]. Deep learning-based

computational pathology methods have been developed to alleviate pathologists’ workload and enhance diagnostic accuracy [1,2,3,4,5]. However, WSIs pose significant challenges due to their giga-pixel scale, resulting in high-dimensional features and complex patterns across multiple scales [11,1,7]. Achieving robust slide-level prediction requires models that can effectively capture both spatial features and global patterns across all regions [8,9,10].

The current approach divides WSIs into small tiles for feature embedding, followed by slide-level models that aggregate these features for WSI predictions [12,6,7]. While this two-stage paradigm enables giga-pixel processing, it struggles with the trade-off between model complexity and the limited availability of WSI data, making overfitting a concern [13]. To address this, Multiple Instance Learning (MIL) samples a subset of tiles and assigns a slide label as the bag-level label. However, due to memory constraints, MIL operates on only a limited set of regions rather than the entire slide, leading to inefficient training and weakly supervised labeling [12,14,16]. Recent methods such as CLAM [15], Gigapath [17], and TransMIL [18] attempt to incorporate spatial relationships by processing more tiles with complex Transformer models, yet key challenges remain unresolved, particularly in scaling to whole-slide inference.

A major challenge is handling the variable number of tiles across WSIs of different scales. While fixed-size sampling or padding strategies enable model training, they hinder full-slide inference as they are not designed for variable input sizes [13]. Transformers offer a potential solution by inherently handle variable sequence lengths; however, their architectural complexity scales with data complexity, increasing the risk of overfitting given the typically limited slide-level data. Furthermore, the local homogeneity and global heterogeneity of pathological features necessitate models capable of capturing both fine-grained details and broader spatial relationships [19]. Consequently, balancing training efficiency with inference performance is critical—models must learn diverse slide-level patterns without excessive complexity while ensuring robust inference across all tiles [10].

Inspired by long-text modeling techniques in large language models, we introduce PathRWKV, a novel recurrent model for pathology image analysis. The Recurrent module is proposed to enable dynamic perceptible tile modeling while enhancing sensitivity to variable tile counts. Moreover, the linear attention from RWKV [20] is employed to reduce computational complexity and mitigate overfitting. Additionally, multi-task learning (MTL) [22] is employed to enhance training efficiency by extracting and integrating diverse pathological patterns in one training procedure. This also improves model’s understanding toward comprehensive features. Finally, the asynchronous structure is designed to ensure comprehensive slide-level predictions with limited training data. Experimental results demonstrate that PathRWKV achieves state-of-the-art performance across multiple WSI datasets, highlighting its robustness and scalability. Overall, our contributions can be summarized as follows:

- We propose a Recurrent module that makes the model robust to variable tile lengths across different WSIs, presenting whole slide level predication.

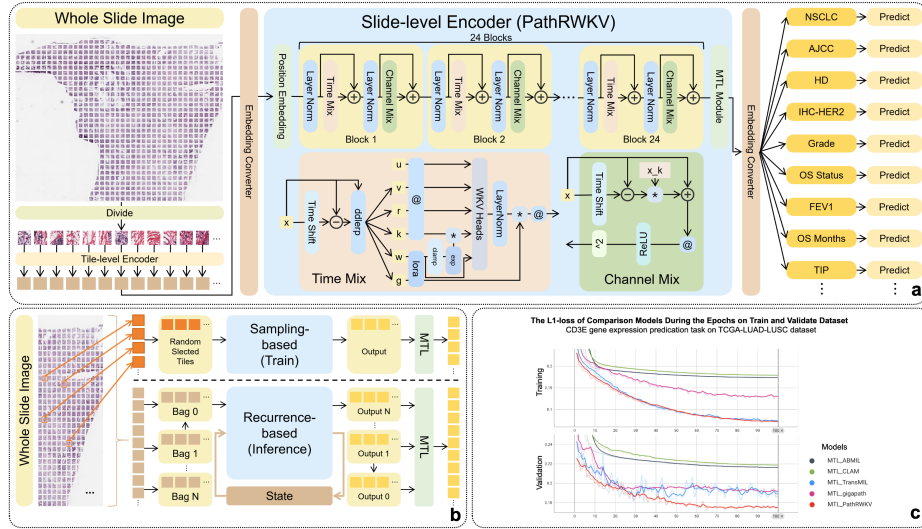


Fig. 1. The overview of (a) PathRWKV pipeline, (b) sampling and recurrence based learning on WSI, and (c) convergence analysis of PathRWKV and others.

- We introduce linear attention to reduce computational complexity and mitigate overfitting.
- We integrate multi-task learning and asynchronous structure design to respectively enhance training efficiency across various clinical indicators and inference performance training on limited data.

2 Methods

Fig.1(a) shows the pipeline with PathRWKV, which will be introduced bottom-top by the sequence of Recurrent, Time Mix and Channel Mix modules in the slide encoder, MTL module after the slide encoder and the data pipeline.

2.1 Slide Encoder

Recurrent Module To enable dynamic perception to iterate all the tiles for each WSI, the slide encoder layers need to explore a recurrent design. Fig.1(b) shows the asynchronous inference design with the Recurrent module, which ensures comprehensive slide-level predictions while training on limited data. During training, the model operates under a parallelized structure, processing a fixed number of maximum tiles from each WSI in a single forward pass. This fully parallelized mechanism maximizes GPU utilization by generating outcomes for all received tiles simultaneously. During inference, the model switches to a recurrent structure to achieve precise results. It processes all tiles from a WSI in a sequential manner, dividing them into multiple bags, each containing the

same number of tiles as used during training. For each bag, the model generates partial outcomes while retaining latent states as memory for processing subsequent bags. Finally, it aggregates all partial outcomes to produce the final result. This asynchronous design enables effective inference across all tiles, striking a balance between computational efficiency and accuracy accompanied with the MTL module. To build up the recurrent module as the slide encoder, inspired by the RWKVv6 [20], Time Mix module and Channel Mix module are implemented.

Time Mix Module By utilizing time-decayed linear attention mechanism, Time Mix module not only equips the model with the ability to handle variable-length data dynamically, but also reduces the risk of overfitting. Specifically, it first fuses two adjacent tiles x_t and x_{t-1} by **Low-Rank Adaptation**(LoRA) and **data-dependent linear interpolation** (DDLerp):

$$\text{LoRA}_i(x) = \lambda_i + \tanh(xA_i)B_i, \quad i \in \{r, k, v, w, g\} \quad (1)$$

$$\text{DDLerp}_i(a, b) = a + (b - a) \odot \text{LoRA}_i(a + (b - a) \odot \mu_x) \quad (2)$$

where μ_x and each λ_i are vectors, A_i and B_i are weight matrices. The difference of the features between the prior tile and present tile is combined with the present tile by LoRA, then linear interpolated into the present tile by DDLerp for receptance, key, value, weight and gate vectors respectively.

Building on the fused features, the model achieves a more robust capability to adapt to variable data lengths by integrating temporal information with spatial features with time-decayed linear attention. This approach also significantly reduces computational complexity from $O(N^2)$ to $O(N)$ by eliminating the need to compute the full $N \times N$ weight matrix:

$$wkv_t = \text{diag}(u) \cdot k_t^\top \cdot v_t + \sum_{i=1}^{t-1} \text{diag} \left(\prod_{j=i+1}^{t-1} w_j \right) \cdot k_i^\top \cdot v_i \quad (3)$$

where wkv_t is the attention score calculated from each head, u is the bonus for the current tile.

Channel Mix Module To emphasize spatial feature utilization by leveraging channel-wise interactions, Channel Mix module refines the spatial representation of features from the Time Mix module. Specifically, Lerp, a simplified DDLerp, generates key and receptance vectors, followed by an element-wise multiplication as a simple attention mechanism:

$$\text{Lerp}_i(a, b) = a + (b - a) \odot \mu_x, i \in \{k, r\} \quad (4)$$

$$o_c = r_c \odot (k_c W_v) \quad (5)$$

In conclusion, the dual focus on temporal and spatial aspects by Time Mix module and Channel Mix module ensures a robust representation of sequential data, while the time-decayed linear attention mechanism maintains computational efficiency and generalization performance.

2.2 MTL Module

The features are then passed into the MTL module to facilitate multi-task learning. Specifically, a linear layer projects the backbone’s output from the shape $[B, N, D]$ to $[B, N, D * T]$, where B is the batch size, N is the number of tiles, D is the embedding dimension, and T is the number of tasks. This projected output is then reshaped into $[B, N, T, D]$ and split along the third dimension into separate tensors for each task with the shape of $[B, N, D]$. Lastly, an MIL module is applied to transform the slide level output features, resulting in final outputs of size $[B, N]$. This design allows the model to efficiently handle multiple downstream tasks simultaneously while maintaining task-specific feature representations, improving the training efficiency.

2.3 PathRWKV Pipeline

Data Pre-processing We establish a pipeline for cropping and embedding as part of WSI pre-processing. During the cropping stage, each WSI is loaded at the desired microns-per-pixel resolution, and the corresponding tile size T_{size} is calculated. The WSI is then divided into a grid of tile arrays $\{T_{1,1}, T_{2,1}, \dots, T_{n,j}\}$. To ensure high-quality tiles, we apply a two-step filtering process: (1) removing tiles with insufficient tissue coverage and (2) eliminating tiles with low pixel variance. This pre-processing pipeline ensures that only relevant and high-quality tiles are retained for downstream analysis.

Tile-level Feature Embedding The pre-processed tiles are then embedded using ROI-level foundational models. The embedded features capture the distilled information of each tile, providing the slide-level model with pre-processed, high-quality data to enhance its learning efficiency and ability to generalize and make accurate predictions.

Slide-level Feature Modeling PathRWKV is the backbone for slide-level feature modeling. During a forward pass, tiles are first augmented with positional embeddings to enhance spatial feature representation, then fed into the model’s blocks. During training, only a subset of tiles from each WSI is loaded as token sequences to optimize training efficiency. During inference, the Recurrent module is activated, allowing the model to process all tiles from a WSI sequentially for optimal performance. When trained with the MTL method, the MTL module projects the outputs into task-specific representations, enabling the model to handle multiple downstream tasks simultaneously for training efficiency [22].

MTL Task Heads and Loss Calculation The outputs from PathRWKV are passed to multiple prediction heads, each corresponding to a specific task. This maximizes the utility of partially annotated samples and mitigates the challenges

of limited fully annotated data. During training, the losses from each task head are aggregated, allowing the model to learn from all tasks concurrently:

$$\mathcal{L}_{total} = \sum_{i=1}^N \mathcal{L}_i \quad (6)$$

where N represents the number of task heads. We employ the Cross-Entropy Loss and the Mean Absolute Error Loss respectively for classification tasks and regression tasks.

Table 1. The performance comparison with SOTA methods on seven downstream datasets. We choose the most representative task for each dataset

Dataset	PANDA	CAMELYON16	TCGA-Lung	TCGA-BLCA	TCGA-UCEC	TCGA-CESC	TCGA-BRCA
Task	Gleason Score	Breast Metastasis	NSCLC	Staging	HistoDx	Grade	OS Months
Metric	Acc. [%]	Acc. [%]	Acc. [%]	Acc. [%]	Acc. [%]	Acc. [%]	Corr.
SlideAve	66.7	69.6	73.4	50.0	84.2	49.1	0.529
SlideMax	62.5	76.0	75.1	53.8	84.2	47.4	0.518
ABMIL	70.9	93.7	75.7	60.2	89.2	50.9	0.449
DSMIL	68.7	86.1	72.8	58.0	87.5	50.9	0.532
Gigapath	72.4	92.2	71.0	52.2	90.0	45.6	0.569
CLAM	70.6	73.4	68.6	52.3	86.7	49.1	0.537
TransMIL	70.0	93.7	73.4	45.5	88.3	43.9	0.504
PathRWKV	74.0	95.3	76.3	62.5	90.0	54.4	0.664

3 Experiments

3.1 Datasets and Downstream Tasks

Seven datasets and corresponding tasks are explored in this paper, covering most of the general WSI-based pathology diagnosis scenarios: **PANDA** [25] contains 10,616 WSIs, with the task **Gleason Score** evaluating the aggressiveness of prostate cancer based on the microscopic appearance of cancer cells. **CAMELYON16** [26] contains 400 WSIs, with the task **Breast Metastasis** classifying the metastatic breast cancer in lymph nodes. **TCGA-Lung**, the combination of TCGA-LUAD and TCGA-LUSC, contains 1,043 WSIs, with the task **NSCLC** predicting the subtypes of non-small cell lung cancer, and the task **FEV1** predicting the percentage of forced expiratory volume in the first-second relative to the reference value after bronchodilator use. **TCGA-BLCA** contains 455 WSIs, with the task **Staging** predicting the AJCC pathologic primary tumor staging that defines tumor size or extent based on AJCC standards. **TCGA-UCEC** contains 566 WSIs, with the task **HistoDx** identifying breast cancer subtypes, such as invasive ductal carcinoma and invasive lobular carcinoma. **TCGA-CESC** contains 279 WSIs, with the task **Grade** grades tumor by evaluating cell differentiation and structure, directly observable in WSIs. **TCGA-BRCA** contains 1,125 WSIs, with the task **OS Months** predicting the overall survival time in months since the initial diagnosis.

3.2 Implementation Details

All models were initialized using the default method without pre-training. Training consisted of a 20-epoch warm-up phase, followed by 80 epochs with a learning rate of $1e-5$ and cosine weight decay reduced to 0.01 times the initial value, using the Adam optimizer. The model weights from the final epoch were saved. A batch size of 4 was used, with a maximum of 2,000 tiles per WSI during training. Notably, during inference, PathRWKV utilizes all tiles from each WSI, while other methods maintain the same settings as during training. Experiments were conducted on 3 RTX A6000 GPUs, with Python 3.10.16, PyTorch 2.4.0, and CUDA 12.1. Additional experimental details are available in the online release.

3.3 Experiment Results

We compared PathRWKV against ABMIL [23], CLAM [15], DSMIL [24], TransMIL [18], and Gigapath [17]. Additionally, we included two basic methods, SlideAve and SlideMax, as baselines. SlideAve generates predictions by averaging the tile-level outputs, while SlideMax selects the tile with the maximum value for prediction. The results are shown in Tab.1, PathRWKV achieves the best performance on seven datasets, with Gleason Score 74.0% on PANDA, Breast Metastasis 95.3% on CAMELYON16, NSCLC 76.3% on TCGA-Lung, Staging 62.5% on TCGA-BLCA, HistoDx 90.0% on TCGA-UCEC, Grade 54.4% on TCGA-CESC, and OS months 0.664 on TCGA-BRCA, demonstrating its superior performance. Fig.1(c) illustrates that methods with more complex model structures, such as TransMIL and Gigapath, exhibit better data fitting during training compared to simpler models like ABMIL and CLAM. However, these complex models are more prone to overfitting and perform worse during validation, indicating a lack of generalization capability. In contrast, PathRWKV strikes a balance between data fitting and generalization. It outperforms simpler models in both training and validation, proving its effectiveness, while also achieving higher performance than more complex models with lower training fitting, highlighting its exceptional generalization capability.

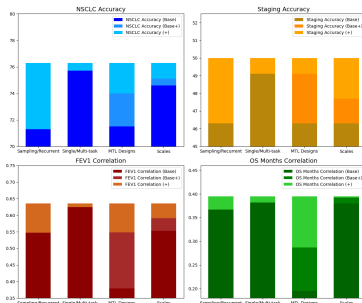
3.4 Ablation Study

All ablation studies are conducted on the TCGA-lung dataset for its large scale and diverse task types, which facilitate a comprehensive evaluation of the model. The results are shown in Tab.2.

Recurrent Module We compare a sampling-based approach same with training, with a recurrence-based approach using our Recurrent module, both sharing identical weights. Results show that our design improves performance across all tasks (NSCLC +5.0%, Staging +3.7%, FEV1 +0.089, OS Months +0.028), proving its improvements in inference performance when using limited training data.

Multi-instance Learning We compare multi-task learning (MTL) with single-task learning (STL). The results indicate that by integrating all tasks into a single process, MTL enhances training efficiency while surpassing STL performance (NSCLC +0.6%, Staging +0.9%, FEV1 +0.012, OS Months +0.013), demonstrating improvements in both training efficiency and inference performance.

Table 2. The ablation studies analyze: 1) Recurrent module: Both structures share weights during inference. The sampling-based structure remains unchanged from training, while the recurrent-based structure uses the Recurrent module to process the full WSI. 2) Multi-task learning: Single-task learning trains each task separately, while multi-task learning trains all tasks together. 3) MTL Module: MTL-Through adds task tokens at the start of the tile sequence. MTL-To transfers tile features to task tokens. MTL-Ours selects the highest-value tile for each task and maps it to the corresponding task head. 4) Model Scaling: B6-D512, B12-D768, and B24-D1024 indicate models with 6, 12, and 24 blocks, with embedding dimensions of 512, 768, and 1024, respectively.



Task	NSCLC	Staging	FEV1	OS Months
Metric	Acc. [%]	Acc. [%]	Corr.	Corr.
Sampling-based	71.3	46.3	0.547	0.367
Recurrent-based	76.3	50.0	0.636	0.395
Single-task Learning	75.7	49.1	0.624	0.382
Multi-task Learning	76.3	50.0	0.636	0.395
MTL-Through	74.0	49.1	0.548	0.287
MTL-None	71.5	46.3	0.379	0.195
MTL-Ours	76.3	50.0	0.636	0.395
B6-D512	74.6	46.3	0.553	0.380
B12-D768	75.1	47.7	0.591	0.392
B24-D1024	76.3	50.0	0.636	0.395

MTL Module To further test the effectiveness of our proposed MTL module, we conduct a comparison experiment between three MTL designs. The results indicate that not all MTL designs are compatible with the model structure. Specifically, compared STL, the MTL-None design underperforms on all tasks, while the MTL-Through design improves performance on some tasks but degrades others. In contrast, our MTL design not only maintains but often surpasses the performance of STL (NSCLC +2.3%, Staging +0.9%, FEV1 +0.088, OS Months +0.108). This underscores the robustness of our MTL module design.

Scale Ability PathRWKV is a Transformer-based model, suggesting it should exhibit strong scalability similar to Transformers, where performance typically improves with more parameters. However, the temporal features in PathRWKV could disrupt this pattern, as traditional RNNs are prone to gradient vanishing or exploding issues when scaled up, potentially hindering scalability. The results

demonstrates that PathRWKV’s scalability is not hindered by its temporal components (NSCLC +1.2%, Staging +2.3%, FEV1 +0.045, OS Months +0.003), and it exhibits strong adaptability to datasets of varying scales.

4 Conclusion

In conclusion, we propose PathRWKV, a novel slide-level model for WSI feature modeling. Specifically, we introduce an advanced architecture that leverages time-decayed linear attention to enhance sensitivity to variable data lengths and reduce the risk of overfitting. Additionally, our asymmetric inference design balances training efficiency and inference performance. PathRWKV effectively addresses the complexity of WSI features while mitigating the challenges posed by limited WSI sample sizes. Extensive experiments across multiple downstream tasks and datasets demonstrate the model’s effectiveness and validate the design objectives.

References

1. Wang, X., Yang, S., Zhang, J., Wang, M., Zhang, J., Huang, J., Yang, W., & Han, X. (2021). TransPath: Transformer-Based Self-supervised Learning for Histopathological Image Classification. In *Medical Image Computing and Computer Assisted Intervention – MICCAI 2021* (pp. 186–195). Cham.
2. Ying, N., Lei, Y., Zhang, T., Lyu, S., Li, C., Chen, S., Liu, Z., Zhao, Y., & Zhang, G. (2023). CPIA Dataset: A Comprehensive Pathological Image Analysis Dataset for Self-supervised Learning Pre-training. *arXiv preprint arXiv:2310.17902*.
3. Zhou, Z., Sodha, V., Siddiquee, M. R., Feng, R., Tajbakhsh, N., Gotway, M. B., & Liang, J. (2019). Models Genesis: Generic Autodidactic Models for 3D Medical Image Analysis. In *Medical Image Computing and Computer Assisted Intervention – MICCAI 2019* (pp. 384–393). Cham.
4. Jamal-Hanjani, M., Wilson, G., Mcgranahan, N., Birkbak, N., Watkins, T., Veeriah, S., Shafi, S., Johnson, D., Mitter, R., Rosenthal, R., Salm, M., Horswell, S., Escudero, M., Matthews, N., Rowan, A., Chambers, T., Moore, D., Turajlic, S., Xu, H., & De Sousa, P. (2017). Tracking the Evolution of Non-Small-Cell Lung Cancer. *New England Journal of Medicine*, 376.
5. Guan, H., & Liu, M. (2022). Domain Adaptation for Medical Image Analysis: A Survey. *IEEE Transactions on Biomedical Engineering*, 69(3), 1173–1185. <https://doi.org/10.1109/TBME.2021.3117407>
6. Zhang, T., Yan, Z., Li, C., Ying, N., Lei, Y., Feng, Y., Zhao, Y., & Zhang, G. (2023). CellMix: A General Instance Relationship based Method for Data Augmentation Towards Pathology Image Classification. *arXiv preprint arXiv:2301.11513*.
7. Zhang, T., Feng, Y., Feng, Y., Zhao, Y., Lei, Y., Ying, N., Yan, Z., He, Y., & Zhang, G. (2022). Shuffle Instances-based Vision Transformer for Pancreatic Cancer ROSE Image Classification. *arXiv preprint arXiv:2208.06833*.
8. Lin, T., Yu, Z., Xu, Z., Hu, H., Xu, Y., & Chen, C. (2023). SGCL: Spatial guided contrastive learning on whole-slide pathological images. *Medical Image Analysis*, 89, 102845. <https://doi.org/10.1016/j.media.2023.102845>

9. Chitnis, S. R., Liu, S., Dash, T., Verlekar, T. T., Di Ieva, A., Berkovsky, S., Vig, L., & Srinivasan, A. (2023). Domain-Specific Pre-training Improves Confidence in Whole Slide Image Classification. *arXiv preprint arXiv:2302.09833*.
10. Quan, H., Li, X., Chen, W., Bai, Q., Zou, M., Yang, R., Zheng, T., Qi, R., Gao, X., Cui, X.: Global Contrast Masked Autoencoders Are Powerful Pathological Representation Learners. arXiv preprint **arXiv:2205.09048** (2022)
11. Hanna, M. G., Parwani, A., Sirintrapun, S. J.: Whole slide imaging: technology and applications. *Advances in Anatomic Pathology* **27**(4), 251–259 (2020)
12. Wang, J., Mao, Y., Guan, N., Xue, C. J.: Advances in Multiple Instance Learning for Whole Slide Image Analysis: Techniques, Challenges, and Future Directions. arXiv preprint **arXiv:2408.09476** (2024)
13. Abdel-Nabi, H., Ali, M., Awajan, A., Daoud, M., Alazrai, R., Suganthan, P. N., Ali, T.: A comprehensive review of the deep learning-based tumor analysis approaches in histopathological images: segmentation, classification and multi-learning tasks. *Cluster Computing* **26**(5), 3145–3185 (2023)
14. Li, J., Li, W., Sisk, A., Ye, H., Wallace, W. D., Speier, W., Arnold, C. W.: A multi-resolution model for histopathology image classification and localization with multiple instance learning. *Computers in Biology and Medicine* **131**, 104253 (2021)
15. Lu, M. Y., Williamson, D. F. K., Chen, T. Y., Chen, R. J., Barbieri, M., Mahmood, F.: Data-efficient and weakly supervised computational pathology on whole-slide images. *Nature Biomedical Engineering* **5**(6), 555–570 (2021)
16. Campanella, G., Hanna, M. G., Geneslaw, L., Mirafior, A., Werneck Krauss Silva, V., Busam, K. J., Brogi, E., Reuter, V. E., Klimstra, D. S., Fuchs, T. J.: Clinical-grade computational pathology using weakly supervised deep learning on whole slide images. *Nature Medicine* **25**(8), 1301–1309 (2019)
17. Xu, H., Usuyama, N., Bagga, J., Zhang, S., Rao, R., Naumann, T., Wong, C., Gero, Z., González, J., Gu, Y., et al.: A whole-slide foundation model for digital pathology from real-world data. *Nature* (2024)
18. Shao, Z., Bian, H., Chen, Y., Wang, Y., Zhang, J., Ji, X., et al.: Transmil: Transformer based correlated multiple instance learning for whole slide image classification. *Advances in Neural Information Processing Systems* **34**, 2136–2147 (2021)
19. Zhang, T., Lyu, S., Lei, Y., Chen, S., Ying, N., He, Y., Zhao, Y., Feng, Y., Lee, H. K., Zhang, G.: PuzzleTuning: Explicitly Bridge Pathological and Natural Image with Puzzles. arXiv preprint **arXiv:2311.06712** (2023)
20. Peng, B., Goldstein, D., Anthony, Q., Albalak, A., Alcaide, E., Biderman, S., Cheah, E., Ferdinan, T., Hou, H., Kazienko, P., et al.: Eagle and finch: Rwkv with matrix-valued states and dynamic recurrence. arXiv preprint **arXiv:2404.05892** (2024)
21. Vaswani, A.: Attention is all you need. *Advances in Neural Information Processing Systems* (2017)
22. Zhang, Y., Yang, Q.: An overview of multi-task learning. *National Science Review* **5**(1), 30–43 (2018)
23. Ilse, M., Tomczak, J., Welling, M.: Attention-based deep multiple instance learning. *International Conference on Machine Learning*, 2127–2136 (2018)
24. Li, B., Li, Y., Eliceiri, K. W.: Dual-stream multiple instance learning network for whole slide image classification with self-supervised contrastive learning. *Proceedings of the IEEE/CVF Conference on Computer Vision and Pattern Recognition*, 14318–14328 (2021)
25. Bulten, W., Kartasalo, K., Chen, P. H. C., Ström, P., Pinckaers, H., Nagpal, K., Cai, Y., Steiner, D. F., Van Boven, H., Vink, R., et al.: Artificial intelligence for

- diagnosis and Gleason grading of prostate cancer: the PANDA challenge. *Nature Medicine* **28**(1), 154–163 (2022)
26. Bejnordi, B. E., Veta, M., Van Diest, P. J., Van Ginneken, B., Karssemeijer, N., Litjens, G., Van Der Laak, J. A. W. M., Hermsen, M., Manson, Q. F., Balkenhol, M., et al.: Diagnostic assessment of deep learning algorithms for detection of lymph node metastases in women with breast cancer. *JAMA* **318**(22), 2199–2210 (2017)